$\sqrt{3}\times\sqrt{3}\rightarrow 6\times 6$ Phase Transition on the Au/Si(111) Surface

J. Nogami, A. A. Baski, and C. F. Quate
E. L. Ginzton Laboratory, Stanford University, Stanford, California 94305
(Received 22 January 1990)

The transition between the $\sqrt{3}\times\sqrt{3}$ and the 6×6 reconstructions of the Au/Si(111) surface is unusual in that, as the Au coverage increases, there is a continuous evolution of the surface structure with Au coverage, rather than a simple change in the relative abundances of two distinct, well-ordered phases. Scanning-tunneling-microscope images show that the $\sqrt{3}\times\sqrt{3}$ structure is broken up into sub-100-Å domains that decrease in size with increasing Au coverage. The 6×6 phase can be described as a periodic arrangement of small $\sqrt{3}\times\sqrt{3}$ domains.

PACS numbers: 61.16.Di, 64.70.Rh, 68.35.Rh

Many metals induce different reconstructions of the Si(111) surface at different metal coverages. In the case of Au, 5×1, $\sqrt{3}\times\sqrt{3}$, and 6×6 phases are seen with increasing coverage up to 2 ML (monolayers).[1] Normally, each metal-induced reconstruction has a well-defined structure characterized by a specific density of metal atoms, and a change in the average metal density on the surface is accommodated by changes in the relative abundance of each phase. In this manner, the surface makes transitions between the different phases with increasing metal coverage.

However, the transition between the Au/Si(111) $\sqrt{3}\times\sqrt{3}$ and 6×6 phases shows anomalous behavior. A previous low-energy electron-diffraction (LEED) study proposed that the $\sqrt{3}\times\sqrt{3}$ structure (hereafter denoted as $\sqrt{3}$) itself is not a perfectly ordered phase, but reflects the local order of a structural subunit of the 6×6 reconstruction.[2] The transition between the $\sqrt{3}$ and the 6×6 structures was viewed as a gradual ordering of $\sqrt{3}$ subunits into a larger 6×6 unit cell. A recent ion-scattering study supports the picture of the $\sqrt{3}$ as being a partially complete 6×6 structure.[3]

Scanning-tunneling-microscope (STM) images of the $\sqrt{3}$ phase support a basic premise of the earlier work: There is a continuous variation with Au coverage in the surface structure between the $\sqrt{3}$ and the 6×6 phases. The novel feature of this transition is that in an intermediate state the surface is not described as a coexistence of distinct, well-ordered $\sqrt{3}$ and 6×6 phases. Instead, the $\sqrt{3}$ structure evolves with coverage, accommodating an excess in Au coverage through the growth of a network of domain walls. Analogous behavior has been studied both experimentally and theoretically in other systems, often involving ordered arrays of gaseous adsorbates on a surface.[4-6] These STM images provide a rare opportunity to observe the microscopic behavior of such a surface phase transition in real space.

All sample preparation and measurement were performed in an ultrahigh-vacuum system with facilities for sample cleaning, annealing, metal deposition, as well as characterization by both LEED and STM.[7] Si wafer samples were cleaned by sputtering or chemical cleaning,[8] and subsequent annealing in vacuum at 1150°C. Au was deposited from a heated tungsten filament, and metal coverages were determined by timed exposure to an evaporant flux previously calibrated by a quartz-crystal microbalance. All samples were prepared by depositing Au at room temperature, annealing 10 min at 700°C, and then slowly cooling to room temperature. LEED and STM measurements were done at room temperature.

The sequence of LEED patterns was as follows: mixed 7×7 and 5×1 for 0–0.4 ML, mixed 5×1 and $\sqrt{3}\times\sqrt{3}$ for 0.5–0.8 ML, "$\sqrt{3}\times\sqrt{3}$" for 0.8–0.95 ML, and 6×6 for 1 ML and above. These coverages agree with those reported by Huang and Williams, in particular assigning about 1 ML to the 6×6 phase.[3] The reproducibility of the LEED results indicated that the relative coverages reported here are accurate to within 0.05 ML.

Figure 1 shows two STM images of the $\sqrt{3}$ structure at 0.8 ML, where the $\sqrt{3}$ dots in the LEED pattern are quite diffuse. These dual-bias images were taken tunneling into and out of the same sample area, thus reflecting empty [Fig. 1(a)] and filled [Fig. 1(b)] states of the sample, respectively. At either bias, the $\sqrt{3}$ structure appears as a centered hexagonal array of bright dots with a typical corrugation of 0.4 Å. The orientation and spacing of the dots is such that one dot appears in each $\sqrt{3}$ unit cell. In this respect, the image is identical to those previously published.[9-11] The interpretation of the image in terms of detailed models of the $\sqrt{3}$ structure will not be addressed here. Many models have been proposed involving either $\frac{2}{3}$- or 1-ML Au coverage; it is not obvi-

(a) (b)

FIG. 1. Two images of the Au/Si(111) $\sqrt{3}\times\sqrt{3}$ structure, taken concurrently with tip bias voltages (a) $V_T=-1.9$ V, (b) $V_T=+0.2$ V, and a tunneling current $I_T=2.7$ nA.

ous which model is supported by these images.[1,3,12]

We focus instead on the interruptions in the periodicity of the $\sqrt{3}$ structure. These appear as white lines in the empty-state image [Fig. 1(a)] consisting of straight segments that run along the sides of the $\sqrt{3}$ unit cell, i.e., along $\langle 11\bar{2}\rangle$ directions. In contrast to the $\sqrt{3}$ features, these boundaries are very different in width and height at the two voltage polarities, indicating that their appearance in the images is not due to topography but is primarily electronic in origin. In the filled-state image [Fig. 1(b)] it is apparent that these boundaries are, at most, one $\sqrt{3}$ unit cell wide, and that the $\sqrt{3}$ structure is undisturbed to either side.

Figure 2(a) shows a portion of the unfilled-state image with a grid superimposed. The registry of the maxima in the $\sqrt{3}$ pattern with the grid shifts across any of the boundaries in the image. As illustrated in Fig. 2(b), this shift indicates that each boundary corresponds to a dislocation of the $\sqrt{3}$ lattice whose Burgers vector is a $[\bar{1}10]$ lattice vector $a = a_0/\sqrt{2}$. As a result, there are three possible domains of the $\sqrt{3}$ structure, all having equivalent registration to the underlying bulk lattice. The existence of such dislocations has been pointed out in previous STM work.[11]

As will be demonstrated, the particular wall configuration shown in Fig. 2(b) not only reproduces the change in registry across a wall, but is also consistent with the behavior of these domain walls with metal coverage. Figure 2(b) is not intended to be a faithful representation of the microscopic structure of the domain wall, however. Images of the wall region show the two rows of $\sqrt{3}$ maxima bordering the wall (indicated by arrows), but not the additional maxima within the wall (shaded circles). The appearance of the wall region is strongly bias dependent, as noted in Fig. 1, but images at low bias show a stripe that is symmetrically placed between the bordering $\sqrt{3}$ maxima (shaded stripe).

The character of these domain walls is more apparent in larger-scale images. Figure 3 shows a sequence of 420-Å square STM images of the surface at coverages between 0.8 and 0.95 ML. These images were taken at negative tip bias where the contrast of the boundaries is high. On this scale the $\sqrt{3}$ structure is no longer visible. Changes in the width or brightness of the domain walls between images are due to varying tip conditions and are not significant. In these images the walls do not appear straight, nor do they intersect in a uniform manner. The average spacing of the walls decreases with increasing coverage.

At coverages less than 0.05 ML above that in Fig. 3(d), both the LEED pattern and the STM images reflect a well-ordered 6×6 surface structure. The rapid changes near the transition to the 6×6 led to situations where a few samples at the same nominal coverage [for example, images 3(c) and 3(d) at 0.95 ML] had significantly different structures. In these cases, for the purposes of this figure, the sequence of coverages was assigned on the basis of the LEED patterns from the samples, after comparison with published patterns and the trends in LEED patterns seen on samples where a gradient in Au density was deliberately introduced. The sharpness of the transition to 6×6 is a reflection of the fact that, as discussed later, the $\sqrt{3}$ phase is able to accommodate excess Au right up to a density very close to that of the 6×6 phase.

Figure 4(a) shows the average domain-wall separation plotted as a function of coverage. This separation was measured by taking the radial distance to the first peaks in the two-dimensional autocorrelation function of large-

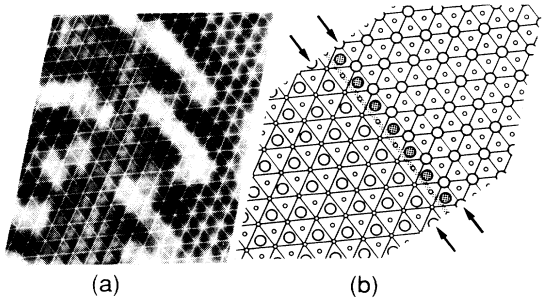

FIG. 2. (a) An image of a domain wall with a superimposed grid. (b) An illustration of a superheavy wall running between the pairs of arrows. Large circles denote the maxima in the $\sqrt{3}\times\sqrt{3}$ structure and smaller circles mark the 1×1 lattice. The shaded line denotes the center of the domain wall.

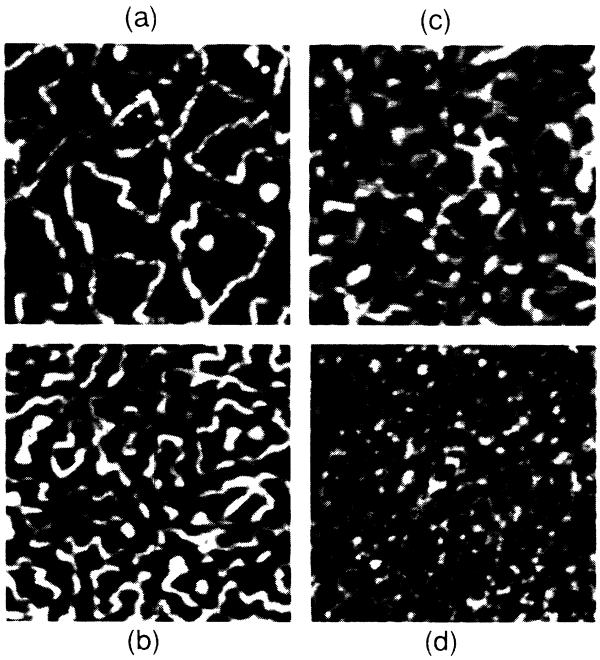

FIG. 3. STM images of samples at various Au coverages (all 420 Å×420 Å). The coverages are (a) 0.8, (b) 0.9, (c) 0.95, and (d) 0.95 ML. All images were taken with V_T between −1.6 and −2 V, and I_T between 0.3 and 1 nA.

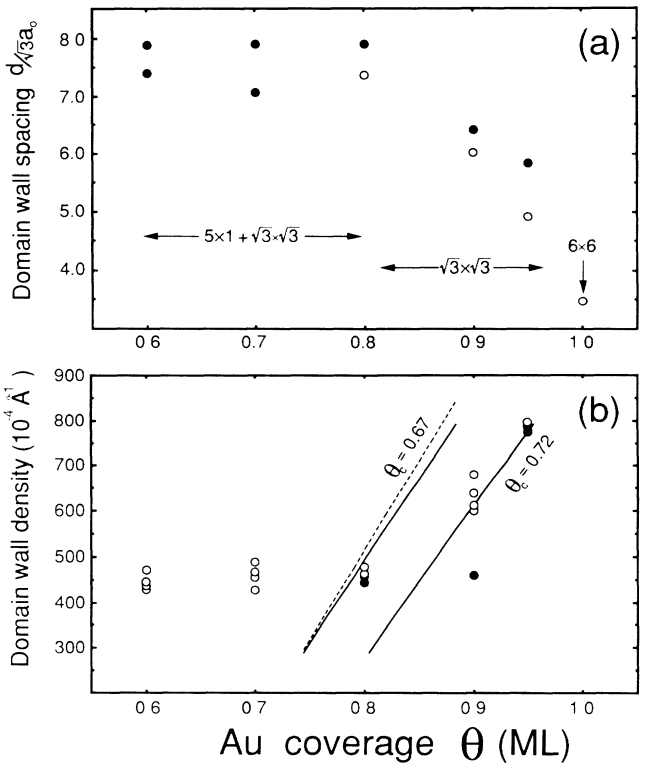

FIG. 4. (a) The average domain-wall spacing, and (b) the density of domain walls, plotted vs coverage. Data for each coverage were obtained on different samples. Like-colored symbols at a given coverage represent measurements in different areas of the same surface. Unlike symbols represent data from different samples. The curves in (b) show calculations for a striped phase (dashed) and a hexagonal phase (solid).

scale images such as those in Fig. 3. Each point is derived from a single image and represents an average over a minimum of 50 domains. The decrease in domain size above 0.8 ML is clearly apparent. In contrast, the domain size remains constant at the lower coverages between 0.6 and 0.8 ML. In this coverage range, the $\sqrt{3}$ phase coexists with the lower-density 5×1 phase, and increases in the gold coverage are accommodated by increasing the proportion of $\sqrt{3}$ on the surface. Also, in this regime, the areas covered by the $\sqrt{3}$ phase are islands several hundred angstroms wide, much larger than the average domain-wall spacing. Above 0.8 ML, the entire surface is covered in $\sqrt{3}$ so that the additional gold must be incorporated in a different manner. The increasing density of domain walls with coverage suggests that the domain walls are associated with a local increase in gold density; i.e., they are heavy domain walls.

It is possible to estimate the increase in gold density per length of domain wall without knowing the explicit structure of the $\sqrt{3}\times\sqrt{3}$ phase. The simplest possible assumption is one in which the $\sqrt{3}$ structure is assumed to continue right up to either side of the wall, and that the wall itself is confined to a single line of $\sqrt{3}$ unit cells that have been contracted in area. There are two simple constructions for such a domain wall, the heavy wall and the superheavy wall.[13] The two types of walls are distinguishable from their associated shifts in registry of the $\sqrt{3}$ lattice. Figure 2(b) models the image in Fig. 2(a) and shows a superheavy wall. Crossing the wall shifts the maxima from on the grid into the centers of triangles pointed away from the wall; a heavy wall would shift the maxima into triangles pointed towards the wall. A similar examination of many images on different samples indicates that almost all the domain walls are of the superheavy type. This preference for only one wall type is also reflected in the shape of the domain walls. When an isolated wall consists of straight $\langle 11\bar{2}\rangle$-oriented sections, all bends in the wall are 60°, a geometry that conserves wall type. A 120° bend in an isolated wall would imply a switch of wall type. Heavy domain walls are seen only at high wall densities, where they run in short segments between wall intersections.

For a striped domain phase, the wall density ρ is

$$\rho=\frac{1}{a}\left[\frac{\theta-\theta_c}{\theta(\frac{1}{2}\Delta A-1)+\theta_c}\right],$$

where $a=3.84$ Å, ΔA is the reduction in area for each unit cell along the domain wall ($\Delta A=1$ for heavy walls and 2 for superheavy walls), and θ_c is the coverage of a pure $\sqrt{3}$ phase. Assuming only superheavy walls, ρ becomes linearly dependent on θ.

Figure 4(b) shows how the domain-wall length per unit area varies with coverage. The domain-wall density is constant until 0.8 ML, whereupon it starts to increase in a roughly linear fashion. Calculated curves are shown for both striped and hexagonal configurations of superheavy walls, for two assumed values of the critical coverage. The hexagonal configuration shows a slight deviation from linearity at high wall densities from the effect of the apexes, but it is clear that calculations for the two different wall topologies give similar results.

For the curves shown, the $\sqrt{3}$ structure is assumed to have $\theta_c\approx\frac{2}{3}$ ML. Overall, the predicted slope is high, which indicates that the assumed gold density along the domain walls is low. This density is strictly prescribed by the assumed structure of the wall, and can be increased beyond what is shown only if the local density of gold is allowed to exceed one Au atom per bulk Si unit cell. The fit to the data is improved if θ_c is allowed to vary 10%, but in truth θ_c is not an adjustable parameter and should be exactly $\frac{2}{3}$ or 1 ML. It is not possible to fit the data with the assumption of $\theta_c=1$ ML, even after allowing for as much as a 30% error in the absolute coverages. It is also difficult to have a realistic configuration for a superheavy domain wall if the $\sqrt{3}$ phase corresponds to 1 ML. The fact that the data curve upward slightly with coverage reflects the production of both superheavy and heavy walls as the wall density increases.

These domain walls break up the long-range order of the $\sqrt{3}$ phase, forming a globally incommensurate struc-

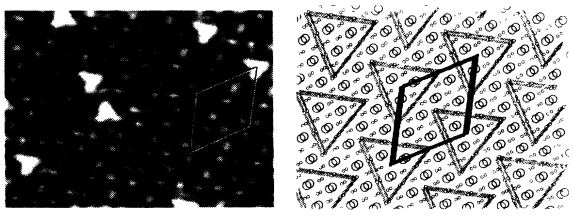

(a) (b)

FIG. 5. (a) An image of the Au/Si(111) 6×6 structure with $V_T = 0.8$ V. One unit cell is outlined. (b) A domain-wall model of the 6×6 structure. Small circles indicate a 1×1 lattice, and larger circles show the positions of maxima in the image. Shaded lines show the domain walls, and the black line outlines a single 6×6 unit cell.

ture. In other examples of incommensurate semiconductor surface structures, there is a misfit between an adsorbate-stabilized surface layer and the underlying bulk, inducing breaks in the structure that have an average periodicity related to the inverse of the misfit.[14-16] The Au/Si(111) $\sqrt{3}$ structure behaves differently in that the average domain size varies strongly with metal density. The formation of domain walls can be viewed as a simple accommodation of the gold in excess of the $\sqrt{3}$ density. The effects of strain are less clear. The constant domain size between 0.6 and 0.8 ML reflects an intrinsic mismatch between the $\sqrt{3}$ surface and the bulk lattice, but its relatively large size implies that the misfit is much smaller than for either Cu or Ga on Si(111).[14,15] The strain associated with domain-wall formation would also appear to be small since the $\sqrt{3}$ structure accommodates a wide range of wall densities and wall configurations.

Figure 5(a) shows an image of the 6×6 structure at 1.0 ML. The most striking feature of the image is the groups of three maxima that have a relative spacing of $\sqrt{3}a$. Since the 6×6 structure is preceded by the convergence of domain walls in the $\sqrt{3}$ structure, it is natural to construct a model of the 6×6 structure in terms of a periodic array of domain walls, as shown in Fig. 5(b). The large circles in Fig. 5(b) correspond to the positions of the maxima in the image and the walls are indicated by shaded stripes in analogy to Fig. 2(b). [The shaded circles in Fig. 2(b) have been omitted here for clarity.] The change in registry across the walls is still consistent with a superheavy wall type. The domain walls form an array of triangular loops. In this configuration, the 6×6 structure consists of subunits that have local $\sqrt{3}\times\sqrt{3}$ structure. This model is only a schematic since the details of the structure depend on the structure that is assumed both for the $\sqrt{3}\times\sqrt{3}$ phase itself and for the domain walls. It should be noted that the images of the 6×6 phase were strongly bias dependent, and were not, in general, describable by this simple model. Most images did exhibit, however, local $\sqrt{3}\times\sqrt{3}$ and $2\sqrt{3}\times2\sqrt{3}$ order as well as a less perfect 6×6 periodicity. Further details of the 6×6 phase will be presented elsewhere.

In summary, STM images demonstrate that the transition with metal coverage between the $\sqrt{3}\times\sqrt{3}$ and the 6×6 reconstructions of the Au/Si(111) surface involves a continuous evolution of the $\sqrt{3}\times\sqrt{3}$ phase. The $\sqrt{3}\times\sqrt{3}$ structure is broken up into sub-100-Å domains that decrease continuously in size as the metal coverage is increased. This progression terminates with the establishment of the 6×6 phase, which can be described in terms of a network of domain walls separating subunits of local $\sqrt{3}\times\sqrt{3}$ order.

This work was supported by the Office of Naval Research. One of the authors (A.A.B.) acknowledges support from AT&T. S. Hosoki kindly provided a preprint of Ref. 11.

[1]G. LeLay, Surf. Sci. **132**, 169 (1983).

[2]K. Higashiyama, S. Kono, and T. Sagawa, Jpn. J. Appl. Phys. **25**, L117 (1986).

[3]J. H. Huang and R. S. Williams, Phys. Rev. B **38**, 4022 (1988).

[4]G. Ertl and P. Rau, Surf. Sci. **15**, 443 (1969).

[5]M. D. Chinn and S. C. Fain, Jr., Phys. Rev. Lett. **39**, 146 (1977).

[6]J. Villain, in *Ordering in Strongly Fluctuating Condensed Matter Systems,* edited by T. Riste (Plenum, New York, 1980).

[7]Sang-il Park and C. F. Quate, Rev. Sci. Instrum. **58**, 2010 (1987).

[8]M. Tabe, Appl. Phys. Lett. **45**, 1073 (1984).

[9]F. Salvan, H. Fuchs, A. Baratoff, and G. Binnig, Surf. Sci. **162**, 634 (1985).

[10]Ph. Dumas, A. Humbert, G. Mathieu, P. Mathiez, C. Mouttet, R. Rolland, F. Salvan, and F. Thibaudau, J. Vac. Sci. Technol. A **6**, 517 (1988).

[11]T. Hasegawa, K. Takata, S. Hosaka, and S. Hosoki, J. Vac. Sci. Technol. A **8**, 241 (1990).

[12]K. Oura, M. Katayama, F. Shoji, and T. Hanawa, Phys. Rev. Lett. **55**, 1486 (1985).

[13]M. Kardar and A. N. Berker, Phys. Rev. Lett. **48**, 1552 (1982); the heavy and superheavy wall notation is used to differentiate between two domain-wall densities of Au and is not to represent the actual structure of the wall. This notation is usually applied to a system where the $\sqrt{3}\times\sqrt{3}$ phase is a $\frac{1}{3}$-ML adsorbate structure.

[14]R. J. Wilson, S. Chiang, and F. Salvan, Phys. Rev. B **38**, 12696 (1988).

[15]D. M. Chen, J. A. Golovchenko, P. Bedrossian, and K. Mortenson, Phys. Rev. Lett. **61**, 2867 (1988).

[16]R. Becker and J. Vickers, J. Vac. Sci. Technol. A **8**, 226 (1990).

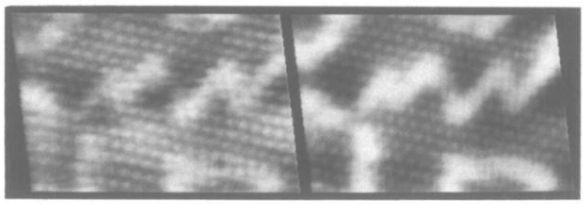

(a) (b)

FIG. 1. Two images of the Au/Si(111) $\sqrt{3}\times\sqrt{3}$ structure, taken concurrently with tip bias voltages (a) $V_T = -1.9$ V, (b) $V_T = +0.2$ V, and a tunneling current $I_T = 2.7$ nA.

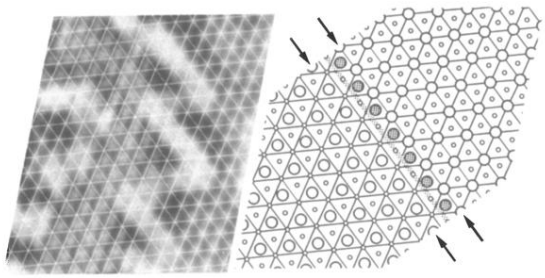

FIG. 2. (a) An image of a domain wall with a superimposed grid. (b) An illustration of a superheavy wall running between the pairs of arrows. Large circles denote the maxima in the $\sqrt{3}\times\sqrt{3}$ structure and smaller circles mark the 1×1 lattice. The shaded line denotes the center of the domain wall.

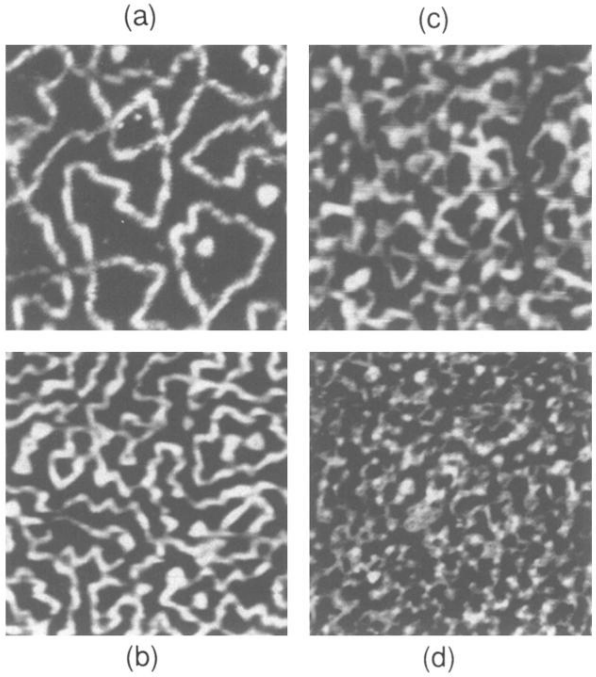

FIG. 3. STM images of samples at various Au coverages (all 420 Å×420 Å). The coverages are (a) 0.8, (b) 0.9, (c) 0.95, and (d) 0.95 ML. All images were taken with V_T between -1.6 and -2 V, and I_T between 0.3 and 1 nA.

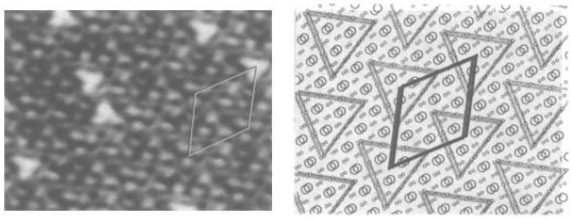

(a) (b)

FIG. 5. (a) An image of the Au/Si(111) 6×6 structure with $V_T = 0.8$ V. One unit cell is outlined. (b) A domain-wall model of the 6×6 structure. Small circles indicate a 1×1 lattice, and larger circles show the positions of maxima in the image. Shaded lines show the domain walls, and the black line outlines a single 6×6 unit cell.